Journal of the Korean Astronomical Society
51: 171 ∼ 183, 2018 December

https://doi.org/10.5303/JKAS.2018.51.6.171
pISSN: 1225-4614 · eISSN: 2288-890X
http://jkas.kas.org

A Golden Decade of Gamma-Ray Pulsar Astronomy†

Chung-Yue Hui[1]
[1]Department of Astronomy and Space Science, Chungnam National University, Daejeon 34134, Korea; cyhui@cnu.ac.kr

Received September 19, 2018; accepted November 14, 2018

Abstract: To celebrate the tenth anniversary since the launch of *Fermi* Gamma-ray Space Telescope, we take a retrospect to a series of breakthroughs *Fermi* has contributed to pulsar astronomy in the last decade. Apart from significantly enlarging the population of $\gamma-$ray pulsars, observations with the Large Area Telescope onboard *Fermi* also show the population is not homogeneous. Instead, many classes and sub-classes have been revealed. In this paper, we will review the properties of different types of $\gamma-$ray pulsars, including radio-quiet $\gamma-$ray pulsars, millisecond pulsars, $\gamma-$ray binaries. Also, we will discuss the prospects of pulsar astronomy in the high energy regime.

Key words: gamma-rays: stars — pulsars: general

1. Introduction

Significant progress in understanding the nature of any class of astronomical objects can be a result of the following key factors: (1) technological breakthrough in instrumentation; (2) systematic sky surveys; (3) multi-wavelength data; and (4) Novel methodologies. In the paper, we will focus on the recent progress in pulsar astronomy as a result of these factors.

Since the discovery of the first pulsar in 1967 (Hewish et al. 1968), the primary driver of progress in pulsar astronomy has been radio observations. A number of extensive radio surveys have led to the discovery of many pulsars. For example, thanks to the innovative 13-beam system receiver (which enlarges the effective area by a factor of 13) Parkes multibeam pulsar survey has discovered $\sim$ 800 pulsars in 1997-2004 (Manchester et al. 2001; Lorimer et al. 2006; Keith et al. 2009). On the other hand, more than one-third of the millisecond pulsars (MSPs), with a spin period $P \lesssim 20$ ms, in globular clusters (GCs) were uncovered by the Green Bank Telescope (Ransom 2008). Once established to be a unique class based on these surveys, meaningful population analyses can be carried out to gain deeper insight on their nature and/or formation processes (e.g., Hui et al. 2010).

We are also interested in the radiation mechanism of these compact objects. While the radio pulsation is the defining characteristic of a pulsar, radio emission typically consumes a small fraction $\sim 10^{-6}$ of the spin-down power $\dot{E} = 4\pi^2 I \dot{P} P^{-3}$ where I is the moment of inertia of the neutron star, P is the rotational period and $\dot{P}$ is the time derivative of P. On the other hand, high energy emission can consume $\sim 10^{-3} - 0.1$ from $\dot{E}$ (e.g., Abdo et al. 2013; Possenti et al. 2002). Therefore, from the energetic point of view, X-ray and $\gamma-$ray observations are better as probes of the acceleration processes in the pulsar magnetospheres.

Once the radio surveys provide the accurate positions of the pulsars by the timing techniques, multi-wavelength follow-up observations can be conveyed. X-ray observations have thus far identified $\sim$ 100 counterparts. Statistical analyses have revealed the correlation between the X-ray luminosities L_x and $\dot{E}$ (e.g., Possenti et al. 2002; Lee et al. 2018). Multiple X-ray emission components have also been identified, which can originate from (1) polar cap heating by return currents from the magnetosphere (appearing as a hard thermal X-ray component), (2) the aforementioned hard thermal X-rays are scattered back to the stellar surface by electrons and re-emitted as a soft X-ray component. and (3) synchrotron radiation from electron/positron pairs (appears as a non-thermal X-ray component) (cf. Cheng et al. 1999)

In the last two decades, many X-ray space telescopes have been launched, including *XMM-Newton*, *Chandra*, *Neil Gehrels Swift* Observatory, *Suzaku* and *NuSTAR*, which have carried out a large number of observations. Apart from targets of planned observations, accumulating archival X-ray data from the fields that are covered by each observation can enable serendipitous counterpart searches (cf. Trepl et al. 2010; Hui et al. 2015a; Lee et al. 2018).

Further up in the energy range ($E > 100$ MeV), our understanding of the properties of pulsars was very limited before 2008. For a long time, our knowledge of their $\gamma-$ray emission was based on a sample of seven pulsars (see Figure 1). Despite the small number, the discovery of $\gamma-$ray pulsars as a group was a remarkable achievement of *Compton* Gamma Ray Observatory (*CGRO*). The main instrument onboard *CGRO* used for studying $\gamma-$ray pulsars is the Energetic Gamma Ray Experiment (*EGRET*) which could detect photons from few tens of MeV to about 10 GeV (Thompson 1993)

There has been a long debate on whether the $\gamma-$rays originate from the acceleration of charged par-

Corresponding author: C. Y. Hui
†Review Article

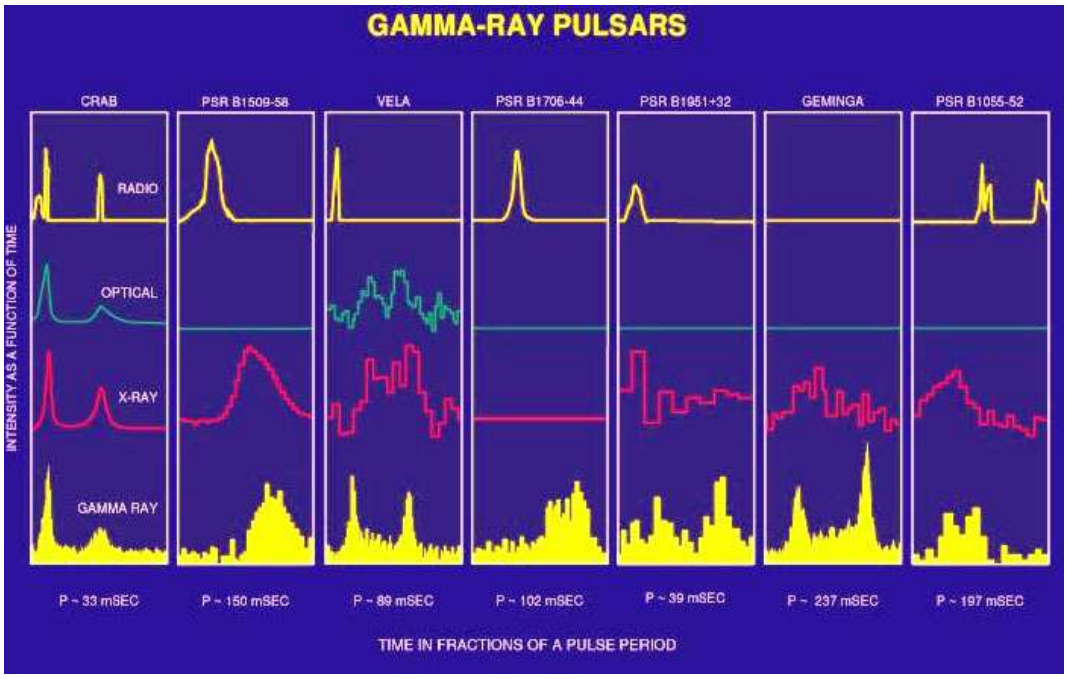

Figure 1. Seven $\gamma-$ray pulsars detected in the *EGRET* era. (Figure courtesy: NASA HEASARC Education and Public Information database, https://heasarc.gsfc.nasa.gov/docs/objects/pulsars/pulsars_lc.html)

ticles near the magnetic pole region (polar cap model) or at the outer magnetosphere (outergap model) (See Cheng et al. 2013; Harding et al. 2013; Song et al. 2016 for a review). Different models predict different $\gamma-$ray properties of pulsars. For example, the polar cap model predicts a $\gamma-$ray spectrum with a very sharp super-exponential cutoff at a few GeV. On the other hand, the outergap model predicts a simple exponential cut-off. As limited by the sample size and the sensitivity of *EGRET* above a few GeV, this debate was unsettled until ten years ago.

2. *Fermi* GAMMA-RAY SPACE TELESCOPE

On 11 June 2008, a satellite initially named as Gamma-ray Large Area Space Telescope (*GLAST*) was launched by a Delta II rocket from Cape Canaveral Air Station. After the successful launch, NASA subsequently renamed it *Fermi* Gamma-ray Space Telescope in honor of the pioneer in high energy physics Enrico Fermi, beginning a new era of high energy astrophysics.

Fermi carries two types of detectors: (1) Large Area Telescope (LAT) and (2) Gamma-ray Burst Monitor (GBM). Both instruments can be seen in Figure 2. In this paper, we are only concerned with LAT as it has been the primary driver behind advances in pulsar astronomy in the last decade.

LAT is a successor of *EGRET* with a much improved instrumental performance and covers an energy range from ~ 100 MeV to ~ 300 GeV. LAT comprises a 4×4 array of identical detection towers. Each tower consists of a tracker (TKR) which is used for reconstructing the incoming direction of the photon and a calorimeter (CAL) which is used for reconstructing the energy of the photon. Each TKR is surrounded by an Anti-Coincidence Detector (ACD), an array of segmented scintillators, which plays a crucial role in background rejection.

When a $\gamma-$ray enters a tower, it will be converted to an electron/positron pair in TKR. While all its predecessors (e.g., *EGRET*, *COS-B*, *SAS-2*) using cross-wire readouts from a gas-filled spark chamber for tracking, the TKR on LAT use a Silicon-Strip Detector (SSD). This significantly improves the accuracy of tracking because there is almost no deadtime as SSD is self-triggering. This leads to improved angular resolution and accuracy in localizing a source.

This is particularly important for multi-wavelength follow-up investigations. For *EGRET*, the positional error box for a typical $\gamma-$ray source is at the order of a degree (cf. Hartman et al. 1999). If you are looking for the X-ray counterpart of a $\gamma-$ray source, several pointings are required to cover the whole $\gamma-$ray box. Furthermore, there can be more than one X-ray source within the error box which complicates the identification. With SSD, LAT is capable of locating a source position with errors at the order of arcminute or sub-arcminute. The improved positional accuracy in $\gamma-$ray is crucial for locating the multi-wavelength counterpart. In some cases, this provides the key to unveil the nature of the $\gamma-$ray sources (see Section 3).

Another major improvement in the instrumental performance of LAT is in its collecting area. LAT's effective area is a function of the photon energy and the off-axis angle. The on-axis effective area of *EGRET* is ~ 1500 cm^2 in the range of $0.2-1$ GeV and drops off at higher and lower energies. For LAT, the effective area

Figure 2. *Fermi* on the ground just before its launch. LAT is the box-shape detector on the top. The GBM detectors and the telemetry antennas can be seen on the left side. On the right side, there is the folded solar panel. (Photo courtesy: NASA FSSC)

is $\sim 7000 - 8000$ cm^2 in $1 - 100$ GeV and the detector response is quite flat in this range.[1] The enlarged area can certainly enhance the capability of finding fainter sources. The discovering power of LAT can be easily illustrated by comparing the $\gamma-$ray source population discovered by it with that discovered by *EGRET*. With ~ 4.5 yrs data collected, *EGRET* identified 271 sources in total (Hartman et al. 1999). On the other hand, using only the first three months of data, LAT has discovered 205 sources with significances $> 10\sigma$ (Abdo et al. 2009a). Besides its large correcting area, the wide energy range covered by LAT also makes it suitable for pulsar studies. This enables us to discriminate the spectral shape predicted by different emission models (e.g., super-exponential cutoff vs. simple exponential cutoff).

With its large field-of-view (> 2 steradians), LAT can scan through the sky efficiently. The spacecraft orbits the earth in ~ 96 minutes, and the whole sky can be surveyed in two orbits. All the data are released and can be accessed through the server run by *Fermi* Science Support Center.[2] Using eight years data, a preliminary LAT source catalog (FL8Y) has recently been released. It includes 5523 sources with significance $> 4\sigma$.

[1] Fermi LAT Performance summary (www.slac.stanford.edu)
[2] https://fermi.gsfc.nasa.gov/ssc/data/access

3. A Zoo of Gamma-Ray Pulsars

Pulsars were in fact the first class of objects identified in the GeV regime. One of the achievements of *Fermi* LAT is in enlarging the population of $\gamma-$ray pulsars significantly (Figure 3). In contrast to the seven pulsars found by *EGRET* in its entire life span (1991–2000), 216 pulsars have been detected by *Fermi* so far.[3]

Fermi also shows us that the $\gamma-$ray pulsar population is far from homogeneous. Many classes of $\gamma-$ray pulsars have been revealed in the last ten years. We will review the properties of each class in the following.

3.1. Millisecond Pulsars

MSPs are characterised by a period $P \lesssim 20$ ms and its derivative $\dot{P} \lesssim 10^{-18}$ s s^{-1}. They are generally thought to be formed when an old neutron star has been spun up by accreting mass and angular momentum from its companion (Alpar et al. 1982; Radhakrishnan & Srinivasan 1982; Fabian et al. 1983). Among the seven $\gamma-$ray pulsars found in the pre-*Fermi* era, none of them is a MSP. Thanks to the much improved sensitivity of LAT, in the second *Fermi* LAT catalog of pulsars (Abdo et al. 2013), 117 $\gamma-$ray pulsars have been listed of which forty are MSPs. By the time of writing, almost ~ 100 of MSPs have been discovered. This makes them the largest class in the $\gamma-$ray pulsar population.

Apart from the improved instrumental performance of LAT, a change of strategy in the search for MSPs also plays a crucial role in enlarging their population (For a detailed review, please refer to Hui 2014). As mentioned in the introduction, radio sky surveys have long been the primary drive for the progress in pulsar astronomy. However, this strategy is limited by the relative small field-of-view of radio telescopes. Since LAT scans through the sky every three hours, its data provide a good coverage of the whole sky. Among a large number of $\gamma-$ray sources uncovered by LAT, one third of them have their nature unidentified/unclassified (cf. Acero et al. 2015). It is not unreasonable to speculate that a fraction of these Unidentified *Fermi* Objects (UFOs) can be MSPs. By applying a set of screening criteria on these UFOs, candidates for MSPs can be selected. For example, Hui et al. (2015a) have chosen seven UFOs for an identification campaign based on the following criteria: (1) high Galactic latitude, (2) absence of $\gamma-$ray variability and (3) spectral shape similar to those of pulsars. Condition 1 was imposed as MSPs are old objects and should be located far away from their birth places (i.e., Galactic plane). Condition 2 was imposed to discriminate them from the active galactic nuclei (AGNs).

LAT can attain a much higher accuracy in positional determination than its predecessor. Searching for the multiwavelength counterparts within the $\gamma-$ray error circles of the candidates selected by the aforementioned procedure turns out to be a efficient way of discovering new MSPs and to pinpoint their nature. For

[3] For updated statistics, see the Public List of LAT-Detected Gamma-Ray Pulsars (confluence.slac.stanford.edu).

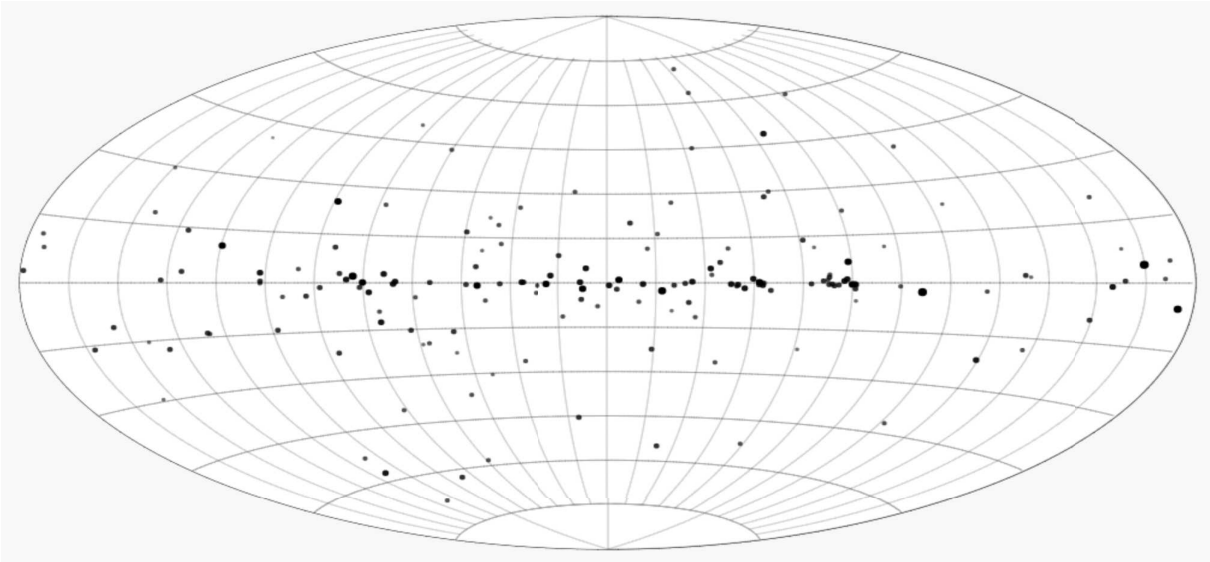

Figure 3. The distribution of 167 $\gamma-$ray pulsars in our Galaxy as detected by *Fermi* LAT with 4 years data. (cf. Acero et al. 2015)

example, most of the UFOs chosen by Hui et al. (2015a) have later been confirmed as MSPs, including the first radio-quiet MSP PSR J1744-7619 (Clark et al. 2018). The timing position of PSR J1744-7619 is consistent with the position of the X-ray counterpart found by Hui et al. (2015a). In some cases, even before the rotational period is found, X-ray/optical observations can almost assure a UFO is indeed a MSP. For example, in the case of 2FGL J2339.6-0532, its counterpart was found to exhibit both X-ray and optical modulation at a periodicity of ~ 4.6 hrs (Kong et al. 2012; Yen et al. 2013). This resembles the orbital modulation found in many MSPs that reside in close binaries. With the discovery of this periodicity, one could be almost certain that 2FGL J2339.6-0532 is a new MSP long before its rotational period of $P \sim 2.88$ ms was discovered (Ray et al. 2014).

The aforementioned strategy of multiwavelength investigations on the MSP-like UFOs has found to be very successful with many MSPs have been identified in this way (e.g., Li et al. 2016; Ng et al. 2016a). We also found that there are various sub-classes of MSPs (See Hui 2014 for a detailed review). Among them, two groups dubbed as "black-widows" and "redbacks" demonstrate the most interesting phenomena.

MSPs are expected to be the end products of the evolution of low-mass X-ray binaries (LMXBs). However, this appears to contradict the observation that $\sim 30\%$ of the known MSPs in the Galactic field are isolated (cf. Hui 2014). For explaining their solitudes, it has been speculated that the high energy radiation and/or the pulsar wind particles from these rejuvenated pulsars have ablated their companions (van den Heuvel & van Paradijs 1988). This is supported by the discovery of MSP PSR B1957+20 which contains a 1.6 ms MSP and a very low mass companion ($M_c \sim 0.02 M_\odot$) in a 9.2 hrs orbit (Fruchter et al. 1988). Eclipses of radio

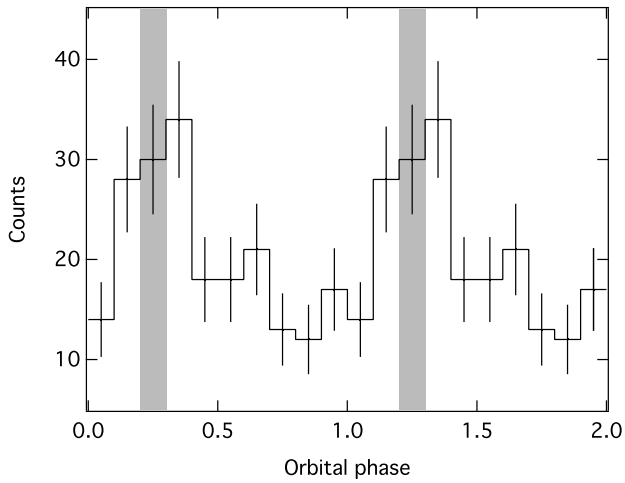

Figure 4. γ-ray light curve of PSR B1957+20 at energies > 2.7 GeV which are folded at the orbital period. Two orbits are shown for clarity. The shaded regions correspond to the phase of radio eclipse. (Wu et al. 2012)

pulsations have been observed when its companion lies between the MSP and us. This indicates the presence of dense ionized gas streaming off from its evaporating companion which absorbs and scatters the radio signals (Kluzniak et al. 1988; Ruderman et al. 1989a,b). PSR B1957+20 is regarded as a prototypical example of "black widow" because the situation is similar to a female spider that eats its companion after mating.

Orbital modulations of PSR B1957+20 at higher energies have also been observed. Optical modulation is observed as the surface of the companion illuminated by the pulsar radiation/wind comes in and out of our light-of-sight (Reynolds et al. 2007; Fruchter et al. 1988; van Paradijs et al. 1988). Huang et al. (2012) have found orbital modulation of the X-ray signal from

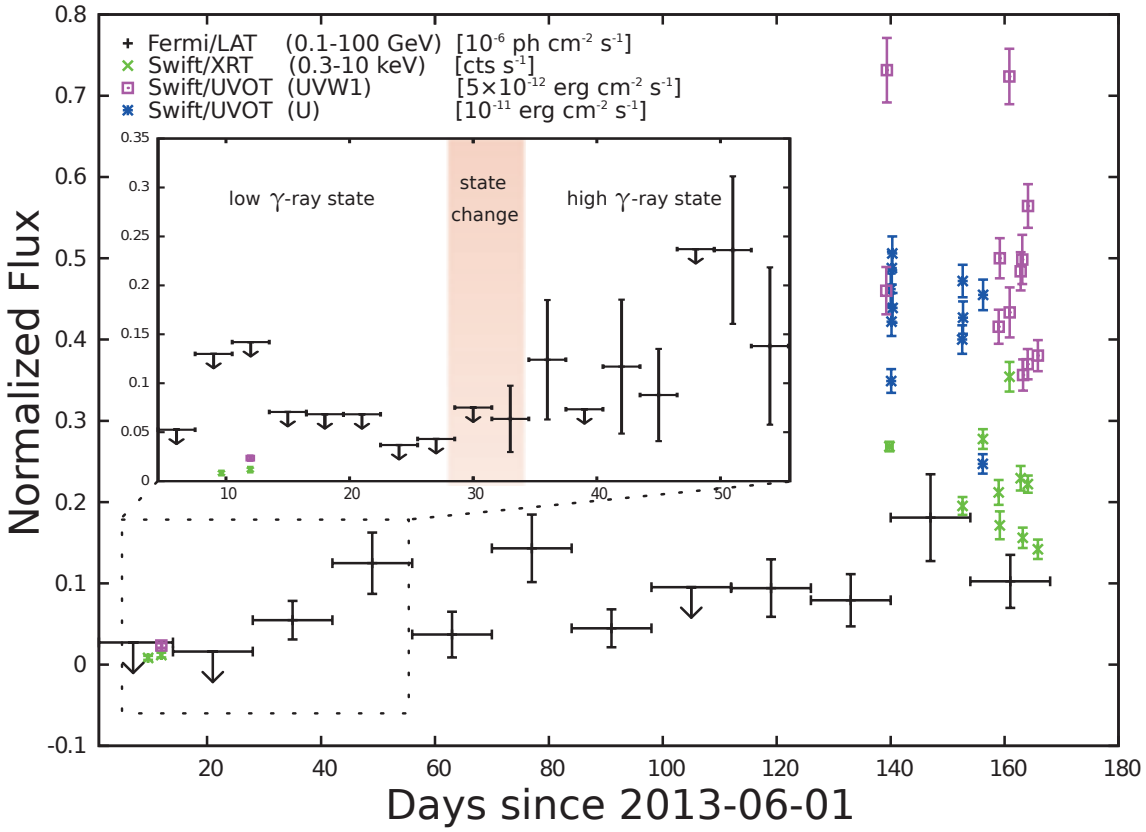

Figure 5. The main panel shows the multi-wavelength (i.e., from UV to γ-ray) lightcurves of PSR J1023+0038 from June 1, 2013 to November 13, 2013 with different flux scales for each energy band (see upper left corner for details) while the inset box indicates the detailed evolution of the γ-ray emissions between June 6 to 24 July. UV/X-ray: Each datum represents an individual observation taken by Swift. γ-ray: Each datum in the main panel (inset) corresponds to two weeks (3 days), and 95% c.l. upper limits are given for the time intervals during which the detection significances is $\lesssim 3\sigma$. (Takata et al. 2014)

PSR B1957+20 which is likely to be originated from the intrabinary shock between the pulsar wind and the ablated material from its companion. We have also discovered an orbital dependence in the γ-ray emission from PSR B1957+20 which can be a result of inverse Compton scattering between the thermal radiation of the companion and the pulsar wind (Wu et al. 2012). The $\gamma-$ray light curve is shown in Figure 4. Thus black widow MSPs can be desirable laboratories for studying the interaction of the radiation and/or wind particles of pulsars with the circumstellar environment. Thanks to the aforementioned multiwavelength investigations of the MSP-like UFOs, ~ 40 black widows have already been found by now.[4]

A new population of eclipsing binary MSPs emerged in the last decade. While their orbital periods are similar to that of black widow MSPs ($P_b \lesssim 20$ hrs), their companion masses ($M_c \sim 0.2 - 0.4 M_\odot$) are larger than that of black widows ($M_c \ll 0.1 M_\odot$). This class is dubbed as "redbacks" (which are the Australian cousins of black widow). These systems can possibly swing between rotation-powered state (i.e., MSP) and accretion-powered state (i.e., LMXB). The prototypical example of this class in the Galactic field is PSR J1023+0038 (Archibald et al. 2009, 2010), which was first identified as a LMXB (Homer et al. 2006) and subsequently as a radio MSP and a former accretion disk was found to disappear (Archibald et al. 2009). Interestingly, since 2013 late June, the radio pulsation of this system has disappeared and a new disk has been formed, which indicates the system has re-entered the accretion-powered state (Stappers et al. 2013; Takata et al. 2014; Li et al. 2014). Accompanying the shift to an accretion active state, our multiwavelength campaign has shown that (1) its $\gamma-$ray flux suddenly increased within a few days in 2013 June/July and has remained at a high $\gamma-$ray state (see Figure 5); (2) both UV and X-ray fluxes have increased by roughly an order of magnitude (see Figure 5); and (3) the spectral energy distribution has changed significantly after the sudden $\gamma-$ray flux change. All these phenomena can be explained by formation of accretion disk result from the sudden increase of stellar wind from the companion. By now, there are ~ 22 redbacks have been found in our Galaxy.

The sample of redbacks and black-widows are large enough for us to further compare their emission prop-

[4] An overview is provided by the Millisecond Pulsar Catalog by A. Patruno (apatruno.wordpress.com)

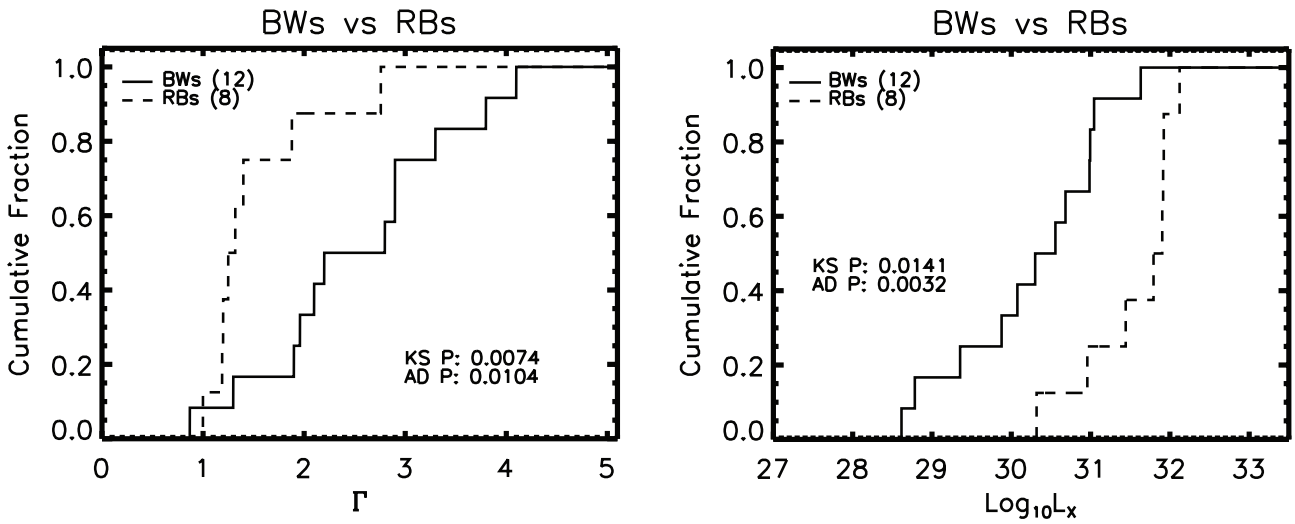

Figure 6. (*Left panel:*) Comparison of the effective photon indices of black-widows (BWs) and redbacks (RBs) in X-ray. (*Right panel:*) Comparison of the X-ray luminosities of BWs and RBs. The $p-$values results from the two-sample Kolmogorov-Smirnov (KS) test and Anderson-Darling (AD) test are given in each figure, which strongly indicate the differences between these two classes of MSPs. (Lee et al. 2018)

erties. In our recent analysis of X-ray properties of MSPs, Lee et al. (2018) found that while the rotational parameters and the orbital periods of redbacks and black-widow are similar, the X-ray emission of redbacks are significantly brighter and harder than that of black-widows (see Figure 6). This can be a result of different contribution of intrabinary shocks in the X-ray emission of these two classes.

3.2. Globular Clusters

Another achievement of *Fermi* LAT is the discovery of $\gamma-$ray emission from globular clusters (GCs) (cf. Tam et al. 2016 and references therein). Owing to the high stellar densities at their cores, GCs are effectively pulsar factories with the production occuring through frequent dynamical interactions (Hui et al. 2010). Over $\sim$ 150 MSPs have been discovered in 28 GCs so far.[5] This is $\gtrsim$ 40% of the known MSP population.

Since MSPs are $\gamma-$ray emitters, GCs are expected to be $\gamma-$ray sources as a collection of a large number of MSPs. Being limited by the sensitivity, *EGRET* did not lead to any positive detection of GCs in the entire span of its mission. However, with only three months data, *Fermi* LAT could already detect GC 47 Tuc at a significance $> 10\sigma$ (Abdo et al. 2009a). Its $\gamma-$ray spectrum resembles that of a pulsar which is characterized by a power-law with an exponential cutoff at $\sim$ 2.5 GeV.

The second $\gamma-$ray GC, Terzan 5, was discovered by Kong et al. (2010) by using $\sim$ 17 months LAT data. Terzan 5 hosts the largest number of detected MSPs (40 up to now). Similar to 47 Tuc, its $\gamma-$ray spectrum as observed by LAT is also characterized by a power-law with an exponential cutoff at a few GeV. With the LAT data accumulated, a whole population of $\gamma-$ray GCs has been established (Abdo et al. 2010; Tam et al. 2011a; Zhou et al. 2016; Zhang et al. 2016; Lloyd et al. 2018). By now, there are 28 GCs have been detected in GeV regime. Among them, NGC 6624 and M28 are special cases.

Individual MSPs are relatively weak $\gamma-$ray emitters with a typical $\gamma-$ray luminosity of $\sim 5 \times 10^{33}$ erg s^{-1} (Tam et al. 2016). Therefore, the MSPs reside in GCs (typically at the distances of few kpc) are difficult to be individually resolved by *Fermi*. However, the very luminous PSR J1823−3021A (in NGC 6624) and PSR B1821-24 (in M28) are exceptions (Freire et al. 2011; Wu et al. 2013). The $\gamma-$ray intensity of these two MSPs are so high that their $\gamma-$ray pulsations have been detected (Figures 7 & 8).

For the other GCs detected by *Fermi*, their $\gamma-$ray emission consists of contributions from the entire MSP population in each cluster. It is interesting to investigate what properties of a GC determine its $\gamma-$ray luminosity. The most obvious factor is the intrinsic number of MSP in a GC which has been found to scale with the two-body encounter rate and the metallicity (Hui et al. 2010). As expected, the $\gamma-$ray luminosities of GCs are found to be strongly correlated with these two parameters (Abdo et al. 2010; Hui et al. 2011; Oh & Hui 2017). Besides the proxies for the MSP population, Hui et al. (2011) have also found that the $\gamma-$ray luminosities of GCs also correlate with the energy densities of optical/IR photons at the cluster location.

This suggests that the $\gamma-$ray emission might be more than just a collection of the magnetospheric emission of the MSPs. According to a scenario of inverse Compton scattering (Cheng et al. 2010), the soft optical/IR photon might serve as seed photons for interactions with the pulsar winds from the MSPs. By combining all these factors, Hui et al. (2011) proposed that fundamental planes can better predict the $\gamma-$ray luminosities of GCs. Figure 9 shows the edge-on view of the

[5] See http://www.naic.edu/~pfreire/GCpsr.html for updated statistics.

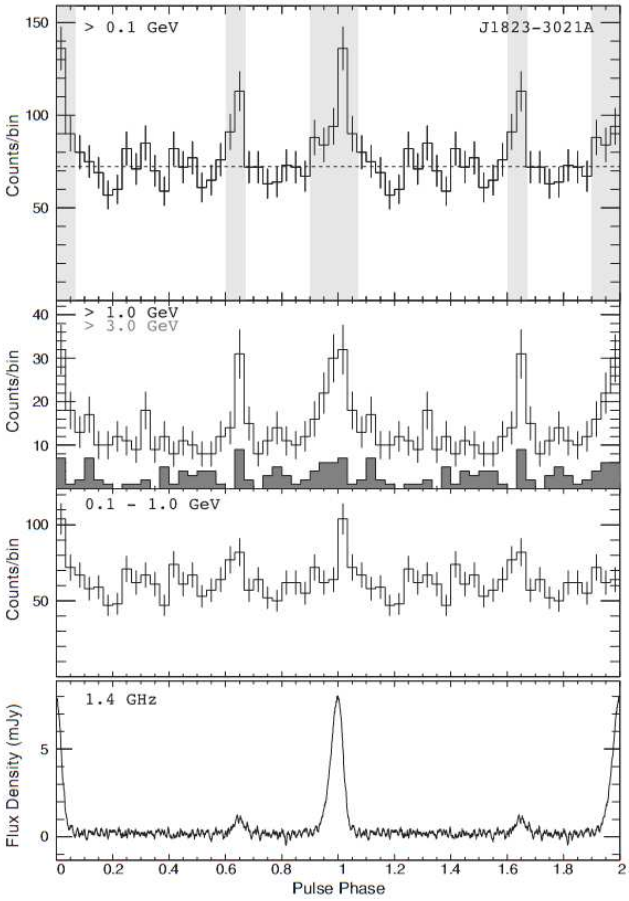

Figure 7. γ-ray and radio pulse profiles of PSR J1823−3021A in the globular cluster NGC 6624. (Freire et al. 2011)

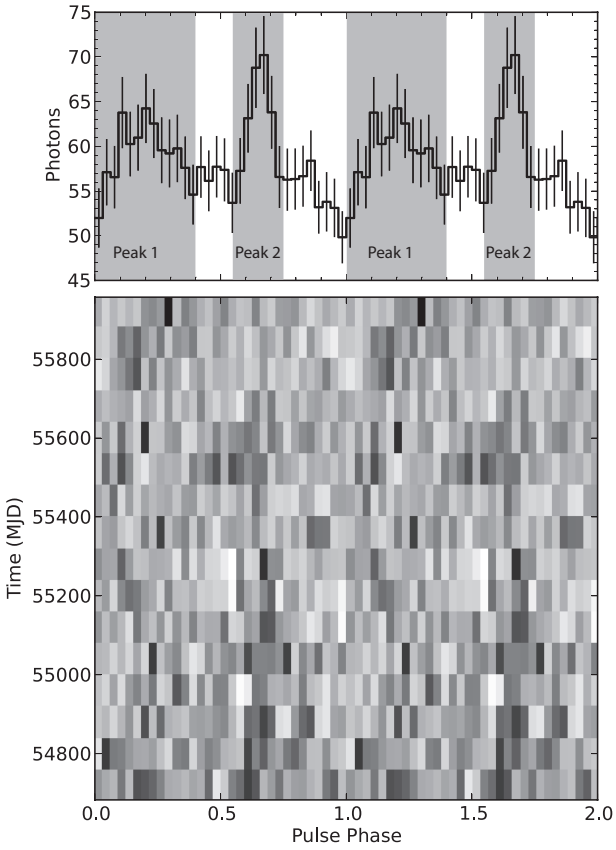

Figure 8. Gamma-ray pulse profile (*upper panel*) and the phaseogram (i.e., the phases of both pulses as a function of time *lower panel*) of PSR B1821-24 in the globular cluster M28. Despite the detection at a significance $> 4\sigma$, the wiggling pulse phases in the phaseogram suggest the presence of inaccuracies in the adopted timing ephermeris. (Wu et al. 2013)

fundamental planes with an updated sample. For the details regarding the updated fundamental plane relations with the enlarged γ−ray GCs sample, please refer to Oh & Hui (2017).

3.3. Radio-Quiet Gamma-Ray Pulsars

Not all the pulsars are detected in radio. The first radio-quiet γ−ray pulsar is the famous Geminga (PSR J0633+1746). Its discovery was a holy grail for the synergy between γ−ray and X-ray observations. The γ−ray emission from Geminga was first detected by the early mission SAS-2 and confirmed by COS-B later (Fichtel et al. 1975). However, due to the limited photon statistics (121 photons detected by SAS-2 in four months) and the large positional error (few degrees at 100 MeV), its nature remained a mystery for almost two decades.

On 13 November 1978, the satellite HEAO-2 was launched and subsequently renamed as *Einstein* X-ray Observatory. *Einstein* was the first X-ray telescope equipped with X-ray focusing optics by means of grazing incidence. Therefore, it was capable of obtaining high resolution X-ray images. Within the γ−ray error box of Geminga as constrained by COS-B, an X-ray source, 1E 0630+178, was identified (Bignami et al. 1983). With much improved positional accuracy constrained by the X-ray observation, multiwavelength investigation could be conducted. 1E 0630+178 turns out to be rather unique. It has a very large X-ray to optical flux ratio of $\sim$ 1000 and no radio counterpart at the X-ray position could be detected by VLA at 6 cm (Bignami et al. 1983). Together with the lack of X-ray temporal variability, Bignami et al. (1983) suggested that it could be a neutron star.

Eventually, coherent X-ray pulsation (0.237 s) from 1E 0630+178 was detected by ROSAT (Halpern et al. 1992). In X-ray regime, there are generally more photons available for the pulsation search. Using the X-ray ephemeris for folding up the γ−ray photons detected by *EGRET*, γ−ray pulsations of Geminga have also been uncovered (Bertsch et al. 1992). Following these discoveries, retrospective analyses of COS-B and SAS-2 data have also identified the same signal (Bignami et al. 1992; Mattox et al. 1992). All these confirmed Geminga as the first radio-quiet γ−ray pulsar. Despite much effort (e.g., Mirabal et al. 2000), no other radio-quiet γ−ray pulsar was found before the launch of *Fermi*. For a long time, Geminga remains to be a very unique source.

The first γ−ray pulsar detected by LAT through

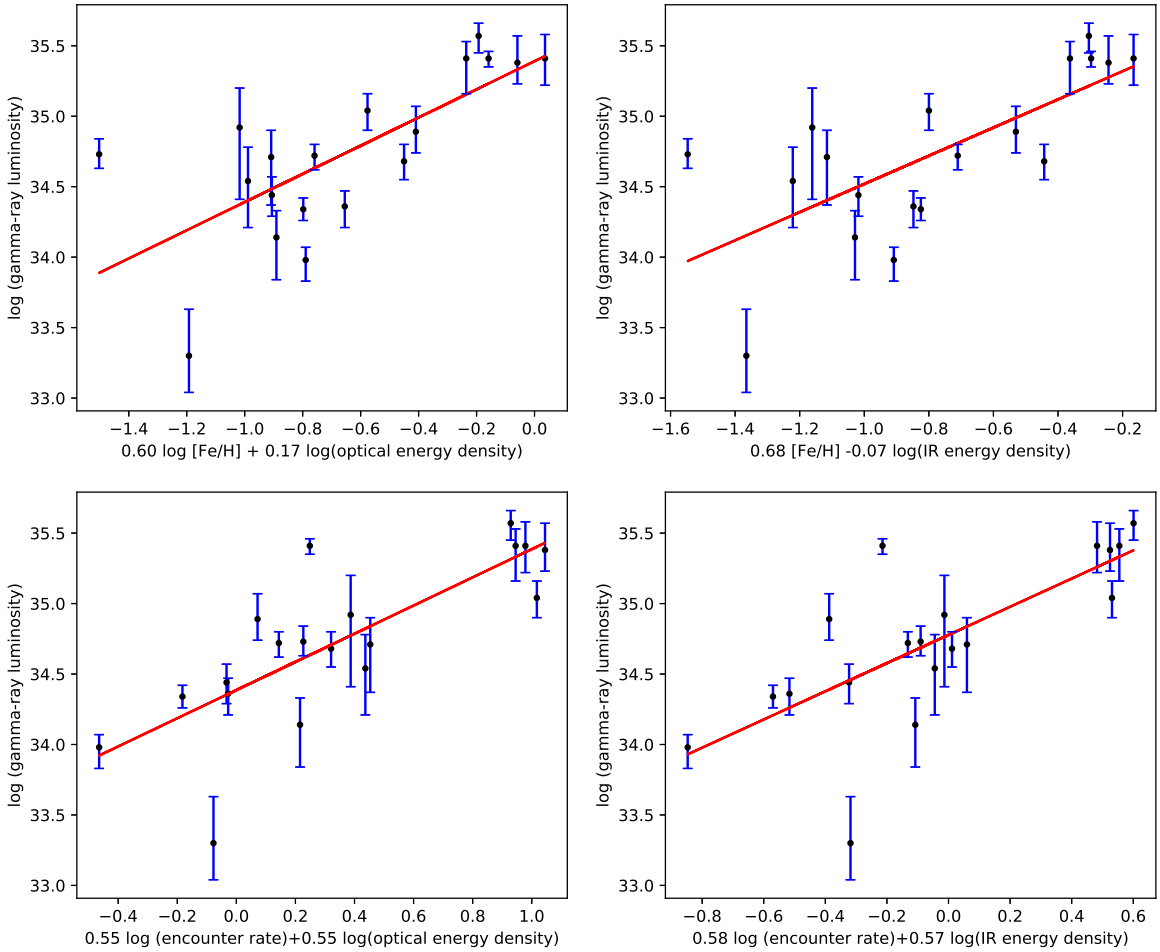

Figure 9. Edge-on views of the fundamental-plane relations of $\gamma-$ray GCs based on the updated sample. (Oh & Hui 2017)

blind search was PSR J0007+7307 associated with the supernova remnant CTA 1 (Abdo et al. 2008). It also turned out to be the long sought radio-quiet $\gamma-$ray pulsar after Geminga. Up to now, more than 40 radio-quiet $\gamma-$ray pulsars have been detected by LAT so far (cf. Hui et al. 2017 and references therein).[6] By now, Geminga is no longer unique. It is only a member of a new class established by *Fermi* (Please refer to Lin et al. 2016 for a detailed review). The population of radio-quiet $\gamma-$ray pulsars is found to be comparable with that of non-recycled radio-loud $\gamma-$ray pulsars. Such a large population of radio-quiet $\gamma-$ray pulsars disfavors the scenario that the $\gamma-$rays are produced from similar regions as those radio emission are radiated (i.e., polar cap regions).

As the sample size of radio-loud and radio-quiet $\gamma-$ray pulsars are now comparable, this allows us to perform meaningful statistical analysis to investigate the differences between these two populations (Hui & Lee 2016; Hui et al. 2017; Yu et al. 2018). The $\gamma-$ray to X-ray flux ratios, magnetic field strength at the light cylinder and the spectral curvature in $\gamma-$rays of these two populations are found to be significantly different (see Figure 10). Though observational effects cannot be ruled out, such differences are not unexpected in the context of the outergap model (see Hui et al. 2017).

[6] The definition of radio-quiet $\gamma-$ray pulsars is their radio fluxes are lower than 30 μJy at 1.4 GHz (Abdo et al. 2013).

3.4. Variable Gamma-Ray Pulsar

PSR J2021+4026 is one of the radio-quiet $\gamma-$ray pulsars found shortly after the operation of *Fermi* LAT commenced (Abdo et al. 2009b). It is a young pulsar with a spin period of $P \sim 265$ ms and a characteristic age of ~ 77 yrs that is associated with the supernova remnant $\gamma-$Cygni (G78.2+2.1) (Trepl et al. 2010; Hui et al. 2015b). Its X-ray counterpart has been identified since the X-ray position corresponds to the optimal timing position found in $\gamma-$ray (Trepl et al. 2010). Its X-ray emission is pulsed and can be attributed to the hot spot on the stellar surface (Lin et al. 2013; Hui et al. 2015b). Besides the thermal emission, non-thermal X-ray component has also been found which can originate from the associated pulsar wind nebula (see Figure 3 in Hui et al. 2015b).

While the $\gamma-$ray emission from pulsars has been long-thought to be stable (see Section 3.1 in this paper), long-term monitoring of PSR J2021+4026 by *Fermi* has

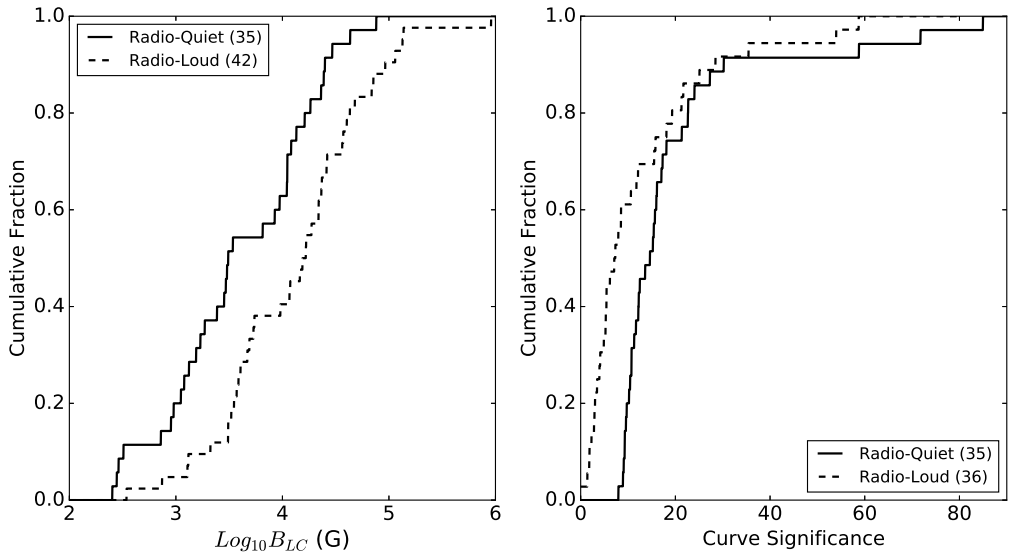

Figure 10. *Left panel:* Comparison of the magnetic field strength at the light cylinders of radio-quiet $\gamma-$ray pulsars and their radio-loud counterparts *Right panel:* Comparison of the $\gamma-$ray spectral curvatures between these two populations. (Hui et al. 2017)

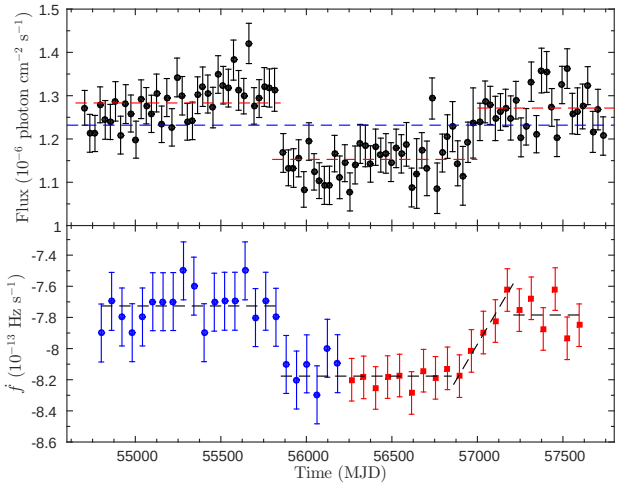

Figure 11. Evolution of $\gamma-$ray flux (*top panel*) and spin-down rate (*bottom panel*) of PSR J2021+4026. A sudden flux jump, which is accompanied by an increase in the spin-down rate, can be seen around the epoch of MJD 55850. The pulsar remained in a lower flux and higher spin-down rate until the epoch around MJD 57000 and then gradually recovered to the pre-glitch stage. (Zhao et al. 2017)

led to a suprise. Around 16 October 2011, a glitch (i.e., a sudden increase in the spin frequency and spin-down rate) was observed (Allafort et al. 2013). Such an event can be a result of a sudden release of stress built in the solid crust of the star or pinned vortices in the superfluid in the stellar interior. Accompanying this glitch, its $\gamma-$ray flux at energy > 100 MeV decreased by $\sim 18\%$ with a significant change in the pulse profile.

Uninterrupted observation with *Fermi* allows follow-up investigations for the post-glitch $\gamma-$ray evolution. Using seven years *Fermi* LAT data, Ng et al. (2016b) show that there is no hint of the $\gamma-$ray flux recovering to the pre-glitch level. They regard this flux change as a permanent effect of this glitch. Moreover, about three years after the aforementioned glitch (around 9 December 2014), Ng et al. (2016b) have noticed another jump in the $\gamma-$ray flux. Zhao et al. (2017) have subsequently shown that both spin-down rate and $\gamma-$ray flux gradually returned to pre-glitch values in a few months after December 2014 (see Figure 11).

It has been speculated that long-term variation can be a result of mode change in the global magnetosphere triggered by the glitch (Ng et al. 2016b; Zhao et al. 2017). Since the magnetic field lines are frozen on the stellar surface, plate tectonic activity triggered by the glitch can lead to a change in the local magnetic field structure around the polar cap and/or the magnetic inclination angle. These can lead to the variation of the electric current circulating in the magnetosphere (Zhao et al. 2017).

To date, PSR J2021+4026 remains to be the only identified variable $\gamma-$ray pulsar.

3.5. Gamma-Ray Binaries

$\gamma-$ray binaries are defined as a class of binary systems emitting $\gamma-$rays in GeV and/or TeV regime and contain a compact object (neutron star/black hole) and a high mass OB companion star (please refer to Dubus et al. 2013 for a detailed review). Their broadband spectral energy distributions (SEDs) are characterized by a peak in νF_ν around GeV and extends to 1-10 TeV bands. This characteristic distinguishes them from the high-mass X-ray binaries (HXMBs) which have their SEDs peak in X-ray regime.

Six systems have so far been confirmed to be $\gamma-$ray binaries: LS I $+61°303$, 1FGL J1018.6-5856, LS 5039, LMC P3, HESS J0632+057 and PSR B1259-63 (cf.

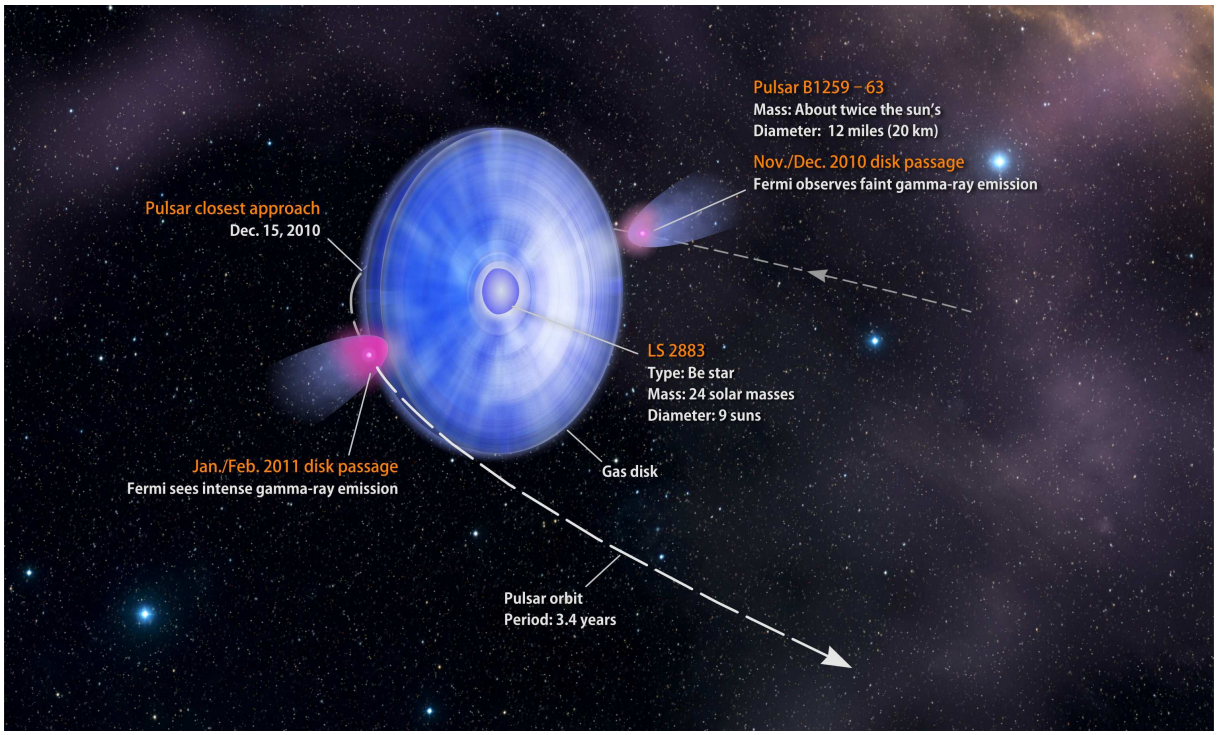

Figure 12. Illustration of the periastron passages of PSR B1259-63/LS2883 as seen in Decemeber 2010. (Illustration: NASA, https://www.nasa.gov/mission_pages/GLAST/news/odd-couple.html)

Dubus et al. 2017 and references therein). Among them, PSR B1259-63 is the only system with the nature of its compact object (pulsar) confirmed.

$\gamma-$ray binaries with a pulsar as a compact object are probably a short-lived stage in the evolution of compact binaries with a massive companion (Tauris & van den Heuvel 2006). They are speculated to be sandwiched between the birth of neutron star and the HMXB phase. As the system evolves, the ram pressure of the accreting material can eventually overcome the pulsar wind which can play a role in extinguishing the pulsar emission. Therefore, a $\gamma-$ray binary turns into a HMXB. Further evolution of its high mass companion will eventually result in the formation of another neutron star/black hole. Therefore, studies of $\gamma-$ray binaries can shed light on the formation paths to double neutron stars and neutron star mergers, which are the sources of short $\gamma-$ray bursts, kilonovae and gravitational wave.

$\gamma-$ray binaries are also ideal laboratories for studying the interaction between the pulsar wind and the stellar wind/radiation from their companions. For instance, PSR B1259-63 has a highly eccentric orbit ($e \sim 0.87$) around a Be star LS2883. Every 3.4 yrs, PSR B1259-63 passes the periastron. It is then not unexpected that the pulsar wind–stellar wind/radiation interaction will strongly depends on the orbital phase. This makes PSR B1259-63 an excellent diagnostic for studying shock physics in a systematically varying environment.

So far *Fermi* LAT has monitored PSR B1259-63/LS2883 for three periastron passages (Tam et al. 2011b, 2015, 2018). The $\gamma-$rays from this system were firstly detected during the 2010 periastron passage (Tam et al. 2011b). The onset of the $\gamma-$ray emission happens close to the phases when the pulsar passes the disk around the Be star. Two major flares were seen around 30 days after the periastron passage (early 2011) which can be a result of Doppler boosting. These processes are illustrated in Figure 12. During the 2014 periastron passage, (Tam et al. 2015) confirmed that these post-periastron GeV flares occured at the similar phases as found in last periastron passage. Moreover, contemporaneous X-ray variabilities with the GeV flare were also found in the 2014 periastron passage. During the most recent periastron passage in 2017, Tam et al. (2018) detected short-lived but powerful GeV flares with time scales down to few hours. The onset of the flaring in 2017 was found to be delayed in comparison with those in 2011 and 2017.

4. FUTURE PROSPECTS IN GAMMA-RAY PULSAR ASTRONOMY

Fermi LAT has definitely enriched our knowledge of the behaviour of $\gamma-$ray pulsars. However, its undesirable instrumental responses at energies $\lesssim 100$ MeV have limited our investigations at soft $\gamma-$rays (i.e., few tens of MeV). While more than 200 pulsars have been uncovered in the GeV regime, the group of soft $\gamma-$ray pulsars remains small (~ 20). A majority of these soft $\gamma-$ray pulsars have hard power-law spectra in hard X-ray regime and attain maxima in MeV range (Kuiper et al. 2015). However, only a small fraction of them

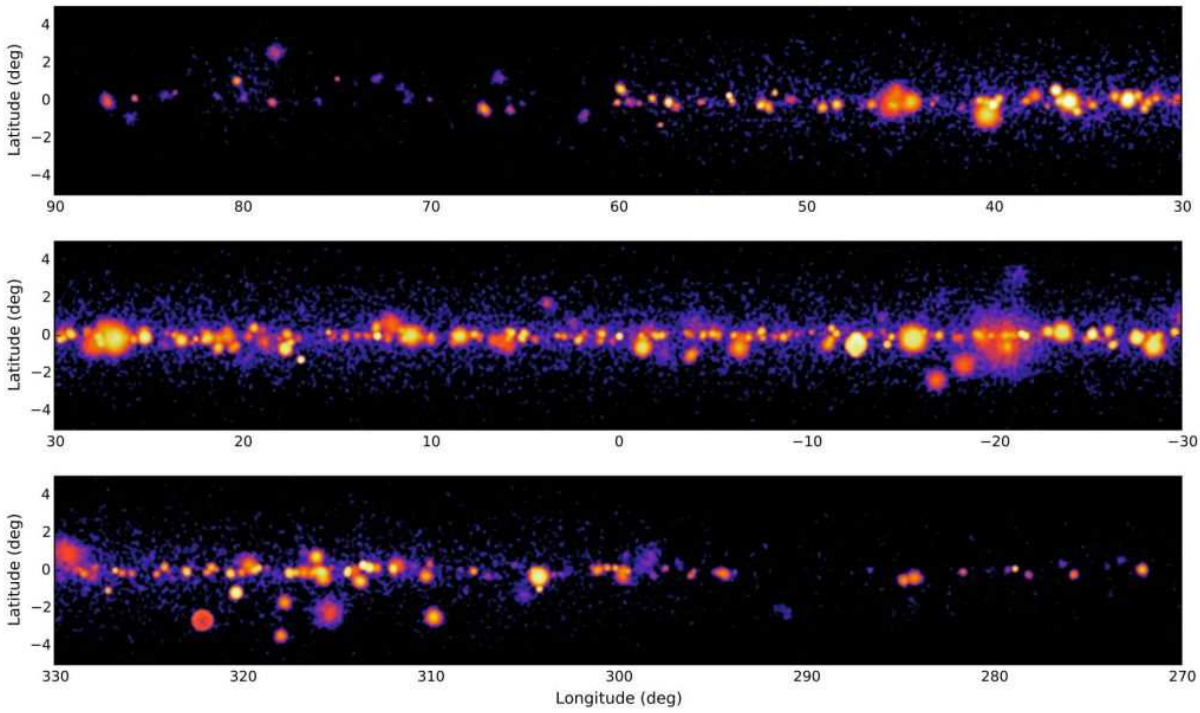

Figure 13. Simulated $\gamma-$ray sky as expected to be observed by CTA during its Galactic plane survey. (Image: CTA Consortium)

have their pulsed emission detected in a GeV regime. One explanation for this phenomena is that the soft $\gamma-$rays and X-rays orginiate from the synchrotron emission radiated by the electron/positron pairs converted from the incoming curvature photons in the presence of strong magnetic field (Wang et al. 2013). For those that have not been detected in GeV band, it is possible that the outgoing current flow misses our line-of-sights.

Studying soft $\gamma-$ray pulsars can thus complement our understanding in pulsar emission mechanisms. And therefore, we would like to enlarge their sample size with observations in hard X-ray and MeV regimes. *NuSTAR* is equipped with focusing optics to image X-rays up to $\sim$ 80 keV. It can help search for the hard X-ray component from the known pulsars. Also the Hard X-ray Modulation Telescope (renamed as *Insight* now) that was launched in 2017 can expand the coverage in hard X-ray band to $\sim$ 250 keV.[7] However, there are no currently operating observatories can cover the MeV and sub-GeV regimes. We have to wait for the planned/proposed facilities in the future (e.g., *PANGU*; Wu et al. 2014).

We have seen that most of the $\gamma-$ray pulsars are characterized by a power-law with an exponential cut-off at a few GeV. Therefore, pulsars in very high energy (VHE; $\gtrsim$ 100 GeV) regime are not expected to be seen. Thus, the detection of pulsed VHE $\gamma-$rays from the Crab pulsar (Aliu et al. 2011) poses challenge to the current pulsar emission models. Very recently, detection of pulsed emission from Vela pulsar with energies up to 80 GeV has been reported (Abdalla et al. 2018). A preliminary VHE detection of pulsed emission from Geminga has just been claimed.[8] All these discoveries have raised important questions about our understanding of the electrodynamics and local environment of pulsars.

In the near future, the next generation VHE observatory, Cherenkov Telescope Array (CTA), will commence its operation. CTA consists of more than 100 telescopes located in both northern and southern hemispheres. In comparison with current instruments, CTA will have a much larger collecting area, wider energy coverage and a larger field-of-view. With the unprecedented performance at such high energies, the source population in the VHE regime is expected to be significantly expanded. Figure 13 shows the simulated results as expected from the CTA Galactic plane survey.[9] About 500 sources are expected to be detected in this survey. It is not unreasonable to speculate that a fraction of these sources can be pulsars. We have good reason to believe that another giant leap of high energy astrophysics is lying ahead!

Acknowledgments

CYH is supported by the National Research Foundation of Korea through grant 2016R1A5A1013277.

References

Abdalla, H., et al. 2018, First Ground-Based Measurement of Sub-20 GeV to 100 GeV γ-Rays from the Vela Pulsar with H.E.S.S. II, A&A, in press (arXiv:1807.01302)

[7] http://www.hxmt.org

[8] Talk of Marcos Lopez at MAGIC 15th Anniversary meeting in June 2018

[9] See https://www.cta-observatory.org for details.

Abdo, A. A., et al. 2008, The Fermi Gamma-Ray Space Telescope Discovers the Pulsar in the Young Galactic Supernova Remnant CTA 1, Science, 322, 1218
Abdo, A. A., et al. 2009a, Fermi/Large Area Telescope Bright Gamma-Ray Source List, ApJS, 183, 46
Abdo, A. A., et al. 2009b, Detection of 16 Gamma-Ray Pulsars Through Blind Frequency Searches Using the Fermi LAT, Science, 325, 840
Abdo, A. A., et al. 2009c, A Population of Gamma-Ray Millisecond Pulsars Seen with the Fermi Large Area Telescope, Science, 325, 848
Abdo, A. A., et al. 2009d, Detection of High-Energy Gamma-Ray Emission from the Globular Cluster 47 Tucanae with Fermi, Science, 325, 845
Abdo, A. A., et al. 2010, A Population of Gamma-Ray Emitting Globular Clusters Seen with the Fermi Large Area Telescope, A&A, 524, A75
Abdo, A. A., et al. 2013, The Second Fermi Large Area Telescope Catalog of Gamma-Ray Pulsars, ApJS, 208, 17
Acero, F., et al. 2015, Fermi Large Area Telescope Third Source Catalog, ApJS, 218, 23
Aliu, E., et al. 2011, Detection of Pulsed Gamma Rays Above 100 GeV from the Crab Pulsar, Science, 334, 69
Allafort, A., et al. 2013, PSR J2021+4026 in the Gamma Cygni Region: The First Variable Gamma-Ray Pulsar Seen by the Fermi LAT, ApJ, 777, L2
Alpar, M. A., Cheng, A. F., Ruderman, M. A., & Shaham, J. 1982, A New Class of Radio Pulsars, Nature, 300, 728
Archibald, A. M., et al. 2009, A Radio Pulsar/X-ray Binary Link, Science, 324, 1411
Archibald, A. M., et al. 2010, X-Ray Variability and Evidence for Pulsations from the Unique Radio Pulsar/X-Ray Binary Transition Object FIRST J102347.6+003841, ApJ, 722, 88
Bertsch, D. L., et al. 1992, Pulsed High-Energy Gamma-Radiation from Geminga (1E0630 + 178), Nature, 357, 306
Bignami, G. F., Caraveo, P. A., & Lamb, R. C. 1983, An Identification for 'Geminga' (2CG 195+04) 1E 0630+178 – A Unique Object in the Error Box of the High-Energy Gamma-Ray Source, ApJ, 272, L9
Bignami, G. F., & Caraveo, P. A. 1992, Geminga: New Period, Old Gamma-Rays, Nature, 357, 287
Cheng, K. S., & Zhang, L. 1999, Multicomponent X-Ray Emissions from Regions near or on the Pulsar Surface, ApJ, 515, 337
Cheng, K. S., Chernyshov, D. O., Dogiel, V. A., Hui, C. Y., & Kong, A. K. H. 2010, The Origin of Gamma Rays from Globular Clusters, ApJ, 723, 1219
Cheng, K. S. 2013, Gamma-Ray Emission from Millisecond Pulsars – An Outergap Perspective, JASS, 30, 153
Clark, C. J., et al. 2018, Einstein@Home Discovers a Radio-Quiet Gamma-Ray Millisecond Pulsar, Science Advances, 4, 7228
Dubus, G., 2013, Gamma-Ray Binaries and Related Systems, A&ARv, 21, 64
Dubus, G., Guillard, N., Petrucci, P.-O., & Martin, P. 2017, Sizing up the Population of Gamma-Ray Binaries, A&A, 608, A59
Fabian, A. C., Pringle, J. E., Verbunt, F., & Wade, R. A. 1983, Do Galactic Bulge X-Ray Sources Evolve into Millisecond Pulsars, Nature, 301, 222
Fichtel, C. E., et al. 1975, High-Energy Gamma-Ray Results from the Second Small Astronomy Satellite, ApJ, 198, 163
Freire, P. C. C., et al. 2011, Fermi Detection of a Luminous Gamma-Ray Pulsar in a Globular Cluster, Science, 334, 1107
Fruchter, A. S., Stinebring, D. R., & Taylor, J. H. 1988, A Millisecond Pulsar in an Eclipsing Binary, Nature, 333, 237
Halpern, J. P., & Holt, S. S. 1992, Discovery of Soft X-Ray Pulsations from the Gamma-Ray Source Geminga, Nature, 357, 222
Harding, A. K. 2013, Pulsar Polar Cap and Slot Gap Models: Confronting Fermi Data, JASS, 30, 145
Hartman, R. C., et al. 1999, The Third EGRET Catalog of High-Energy Gamma-Ray Sources, ApJS, 123, 79
Hewish, A., Bell, S. J., Pilkington, J. D. H., Scott, P. F., & Collins, R. A. 1968, Observation of a Rapidly Pulsating Radio Source, Nature, 217, 709
Homer, L., et al. 2006, XMM-Newton and Optical Follow-Up Observations of SDSS J093249.57+472523.0 and SDSS J102347.67+003841.2, AJ, 131, 562
Huang, R. H. H., et al. 2012, X-Ray Studies of the Black Widow Pulsar PSR B1957+20, ApJ, 760, 92
Hui, C. Y., Cheng, K. S., & Taam, R. E. 2010, Dynamical Formation of Millisecond Pulsars in Globular Clusters, ApJ, 714, 1149
Hui, C. Y., et al. 2011, The Fundamental Plane of Gamma-Ray Globular Clusters, ApJ, 726, 100
Hui, C. Y. 2014, Spider Invasion Across the Galaxy, JASS, 31, 101
Hui, C. Y., et al. 2015a, Searches for Millisecond Pulsar Candidates among the Unidentified Fermi Objects, ApJ, 809, 68
Hui, C. Y., et al. 2015b, A Detailed X-Ray Investigation of PSR J2021+4026 and the Gamma-Cygni Supernova Remnant, ApJ, 799, 76
Hui, C.-Y., & Lee, J. 2016, On the Spectral Shape of Non-Recycled Gamma-Ray Pulsars, JASS, 33, 101
Hui, C. Y., Lee, J., Takata, J., Ng, C. W., & Cheng, K. S. 2017, Differences between Radio-Loud and Radio-Quiet Gamma-Ray Pulsars as Revealed by Fermi, ApJ, 834, 120
Keith, M. J., et al. 2009, Discovery of 28 Pulsars Using New Techniques for Sorting Pulsar Candidates, MNRAS, 395, 837
Kong, A. K. H., Hui, C. Y., & Cheng, K. S. 2010, Fermi Discovery of Gamma-Ray Emission from the Globular Cluster Terzan 5, ApJ, 712, L36
Kong, A. K. H., et al. 2012, Discovery of an Unidentified Fermi Object as a Black Widow-Like Millisecond Pulsar, ApJ, 747, L3
Kluzniak, W., Ruderman, M., Shaham, J., & Tavani, M. 1998, Nature and Evolution of the Eclipsing Millisecond Binary Pulsar PSR1957 + 20, Nature, 334, 225
Kuiper, L., & Hermsen, W. 2015, The Soft Gamma-Ray Pulsar Population: A High-Energy Overview, MNRAS, 449, 3827
Lee, J., et al. 2018, X-Ray Census of Millisecond Pulsars in the Galactic Field, ApJ, 864, 23
Li, K. L., et al. 2014, NuSTAR Observations and Broadband Spectral Energy Distribution Modeling of the Millisecond Pulsar Binary PSR J1023+0038, ApJ, 797, 111
Li, K.-L., et al. 2016, Discovery of a Redback Millisecond Pulsar Candidate: 3FGL J0212.1+5320, ApJ, 833, 147
Lin, L. C. C., et al. 2013, Discovery of X-Ray Pulsation from the Geminga-Like Pulsar PSR J2021+4026, ApJ, 770, L9
Lin, L. C.-C. 2016, Radio-Quiet Gamma-Ray Pulsars, JASS, 33, 147

Lloyd, S. J., Chadwick, P. M., & Brown, A. M. 2018, Gamma-Ray Emission from High Galactic Latitude Globular Clusters, MNRAS, 480, 4782
Lorimer, D. R., et al. 2006, The Parkes Multibeam Pulsar Survey – VI. Discovery and Timing Of 142 Pulsars and a Galactic Population Analysis, MNRAS, 372, 777
Manchester, R. N., et al. 2001, The Parkes Multi-Beam Pulsar Survey – I. Observing and Data Analysis Systems, Discovery And Timing Of 100 Pulsars, MNRAS, 328, 17
Mattox, J. R., et al. 1992, SAS 2 Observation of Pulsed High-Energy Gamma Radiation from Geminga, ApJ, 401, L23
Mirabal, N., Halpern, J. P., Eracleous, M., & Becker, R. H. 2000, Search for the Identification of 3EG J1835+5918: Evidence for a New Type of High-Energy Gamma-Ray Source, ApJ, 541, 180
Ng, C.-W., Cheng, K.-S., & Takata, J. 2016a, Exploring the Extra Component in the Gamma-Ray Emission of the New Redback Candidate 3FGL J2039.6-5618, JASS, 33, 93
Ng, C. W., Takata, J., & Cheng, K. S. 2016b, Observation and Simulation of the Variable Gamma-Ray Emission from PSR J2021+4026, ApJ, 825, 18
Oh, K., & Hui, C. Y. 2017, Reexamining the gamma-Ray Properties of Globular Clusters, Proceedings of the 7th International Fermi Symposium, Held 15-20 October 2017, in Garmisch-Partenkirchen, Germany (IFS2017), id.106
Possenti, A., Cerutti, R., Colpi, M., & Mereghetti, S. 2002, Re-Examining the X-Ray versus Spin-Down Luminosity Correlation of Rotation Powered Pulsars, A&A, 387, 993
Radhakrishnan, V., & Srinivasan, G. 1982, On the Origin of the Recently Discovered Ultra-Rapid Pulsar, Current Science, 51, 1096
Ransom, S. M. 2008, Dynamical Evolution of Dense Stellar Systems, Proceedings of the International Astronomical Union, IAU Symposium, Volume 246, 291
Ray, P. S., et al. 2014, Discovery of the Radio and Gamma-Ray Pulsar PSR J2339-0533 Associated with the Fermi LAT Bright Source 0FGL J2339.8-0530, AAS, AAS Meeting #223, id.140.07
Reynolds, M. T., et al. 2007, The Light Curve of the Companion to PSR B1957+20, MNRAS, 379, 1117
Ruderman, M., Shaham, J., & Tavani, M. 1989a, Accretion Turnoff and Rapid Evaporation of Very Light Secondaries in Low-Mass X-Ray Binaries, ApJ, 336, 507
Ruderman, M., Shaham, J., Tavani, M., & Eichler, D. 1989b, Late Evolution of Very Low Mass X-Ray Binaries Sustained by Radiation from Their Primaries, ApJ, 343, 292
Song, Y., Cheng, K. S., & Takata, J. 2016, Theoretical Study of Gamma-Ray Pulsars, JASS, 33, 69
Stappers, B. W., et al. 2013, State-Change in the "Transition" Binary Millisecond Pulsar J1023+0038, ATel, 5513
Takata, J., et al. 2014, Multi-Wavelength Emissions from the Millisecond Pulsar Binary PSR J1023+0038 during an Accretion Active State, ApJ, 785, 131
Tam, P. H. T., et al. 2011a, Gamma-Ray Emission from the Globular Clusters Liller 1, M80, NGC 6139, NGC 6541, NGC 6624, and NGC 6752, ApJ, 729, 90
Tam, P. H. T., et al. 2011b, Discovery of GeV Gamma-Ray Emission from PSR B1259-63/LS 2883, ApJ, 736, L10
Tam, P. H. T., et al. 2015, High-Energy Observations of PSR B1259-63/LS 2883 through the 2014 Periastron Passage: Connecting X-Rays to the GeV Flare, ApJ, 798, L26
Tam, P,-H. T., Hui, C. Y., & Kong, A. K. H. 2016, Gamma-Ray Emission from Globular Clusters, JASS, 33, 1
Tam, P. H. T., He, X.-B., Pal, P. S., & Cui, Y. 2018, The Hour-Timescale GeV Flares of PSR B1259-63 in 2017, ApJ, 862, 165
Tauris, T. M., & van den Heuvel, E. P. J. 2006, Formation and Evolution of Compact Stellar X-Ray Sources, Compact Stellar X-Ray Sources, edit. by Walter Lewin & Michiel van der Klis, Cambridge Astrophysics Series (Cambridge: Cambridge University Press), 39
Thompson, D. J. 1993, Timing Analysis of EGRET/CGRO Data, Isolated Pulsars, Proceedings of the Los Alamos workshop (in New Mexico on February 23-28, 1992), edited by K. A. Riper, R. Epstein and C. Ho. (Cambridge: Cambridge University Press), 385
Trepl, L., et al. 2010, Multiwavelength Properties of a New Geminga-Like Pulsar: PSRJ2021+4026, MNRAS, 405, 1339
van den Heuvel, E. P. J., & van Paradijs, J. 1988, Fate of the Companion Stars of Ultra-Rapid Pulsars, Nature, 334, 227
van Paradijs, J., et al. 1988, Optical Observations of the Eclipsing Binary Radio Pulsar PSR1957+20, Nature, 334, 684
Wang, Y., Takata, J., & Cheng, K. S. 2013, Mechanism of the X-Ray and Soft Gamma-Ray Emissions from the High Magnetic Field Pulsar: PSR B1509-58, JASS, 30, 91
Wu, E. M. H., et al. 2012, Orbital-Phase-Dependent Gamma-Ray Emissions from the Black Widow Pulsar, ApJ, 761, 181
Wu, J. H. K., et al. 2013, Search for Pulsed Gamma-Ray Emission from Globular Cluster M28, ApJ, 765, L47
Wu, X., et al. 2014, PANGU: A High Resolution Gamma-Ray Space Telescope, arXiv:1407.0710
Yen, T.-C., et al. 2013, Optical and Infrared Lightcurve Modeling of the Gamma-Ray Millisecond Pulsar 2FGL J2339.6-0532, JASS, 30, 159
Yu, H.-F., Hui, C., Ye, K., Albert, K. H., & Takata, J. 2018, Bayesian Inference on the Radio-Quietness of Gamma-Ray Pulsars, ApJ, 857, 120
Zhang, P. F., et al. 2016, Detection of Gamma-Ray Emission from Globular Clusters M15, NGC 6397, 5904, 6218 and 6139 with Fermi-LAT, MNRAS, 459, 99
Zhao, J., et al. 2017, Mode Change of a Gamma-Ray Pulsar, PSR J2021+4026, ApJ, 842, 53
Zhou, J. N., et al. 2015, Gamma-Ray Emission from Globular Clusters 2MS-GC01, IC 1257, FSR 1735, NGC 5904 and 6656, MNRAS, 448, 3215